

Presentation at the 2014 meeting on Topical Problems of Nonlinear Wave Physics, Nizhniy Novgorod–Saratov—Nizhniy Novgorod, Russia

July 17–23, 2014

Reconstructing sea-level pressure variability via a feature-tracking approach

S. Kravtsov^{1,2}, I. Rudeva^{3,2}, and S. K. Gulev²

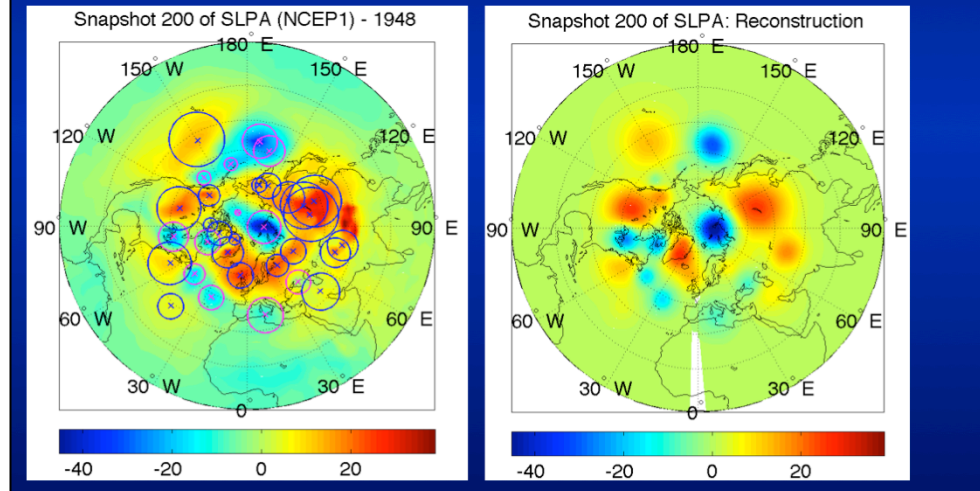
¹ University of Wisconsin-Milwaukee, Department of Mathematical Sciences, Atmospheric Science Group

² P. P. Shirshov Institute of Oceanology, Russian Academy of Sciences, Moscow, Russia

³ Department of Earth Sciences, University of Melbourne, AU
<http://www.uwm.edu/kravtsov/>

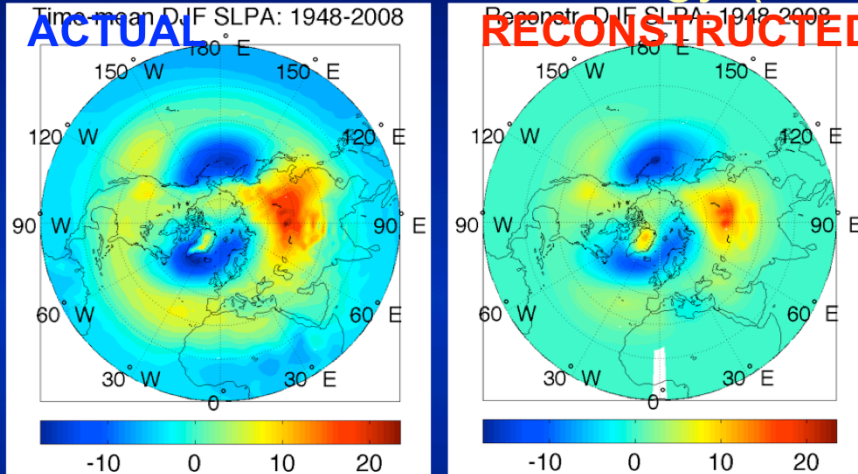
Synoptic field reconstruction

Identify cyclones (SLP minima) and anticyclones (SLP maxima) — approximate with axially symmetric Gaussians — reassemble synoptic field



Snapshots of sea-level pressure are dominated in mid-latitude regions by synoptic-scale features known as cyclones (SLP minima) and anticyclones (SLP maxima). These features have lifetimes on the order of a few days, propagate and bring about what we all know as ever-changing weather. They may also be important in forcing and modifying low-frequency climate variability (LFV), with time scales longer than a week and spatial scales from regional to global. Traditional way of singling out this synoptic field is via high-pass time filtering. However, it turns out that the spectrum of atmospheric variability is continuous and monotonic, so there is no clear time scale separation between synoptic field and LFV. What we propose here is an alternative strategy of isolating the synoptic field based on identifying and tracking the evolution of individual cyclones and anticyclones. In particular, we identify locations of all cyclones and anticyclones present in a given SLP snapshot, and approximate the actual SLP maxima and minima by positive and negative axially symmetric anomalies of Gaussian shape, with size and depth derived from the observed field (see the left panel). We then sum up all these anomalies to create a reconstructed synoptic field for each SLP snapshot (right panel); this field essentially has the large-scale background removed. The main question we attempt to address is: “How well the synoptic field so reconstructed describes the total variability present in the raw SLP field?” What we will find is that this synoptic field describes a perhaps surprisingly large fraction of the total SLP variability, including most of its LFV!

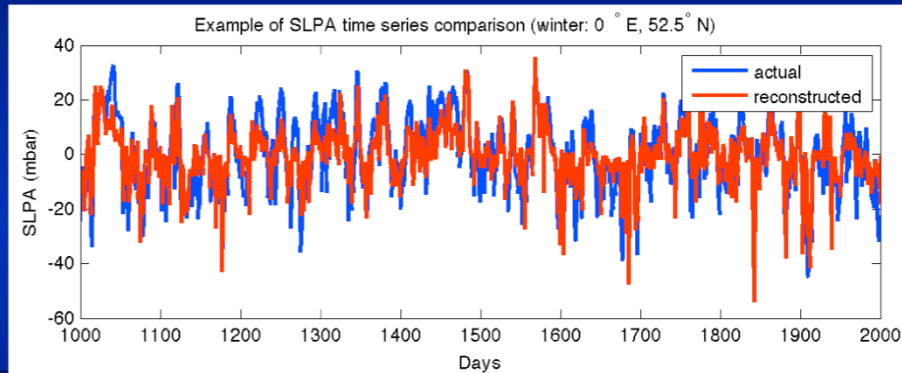
Reconstructed Climatology (DJF)



- Decent spatial correlations
- Reconstr. underestimates land-sea contrast
- Larger discrepancies toward south

Now that we have the full and synoptically reconstructed field we can compare their various spatiotemporal characteristics, the simplest of which is the long-term time mean. Shown in the left panel is the SLP climatology in winter season (DJF) for the full SLP field [rather, the deviation of SLP from the basin-average value], while in the right panel — the same quantity for the synoptically reconstructed field. The two fields are apparently well correlated, although the synoptic field underestimates the land-sea contrast present in the full field and exhibits progressively weaker deviations from the basin mean in the subtropical regions. The latter property may at least partly be due to the fact that our tracking scheme concentrates on the mid-latitude regions and does not include tropical cyclones and anticyclones.

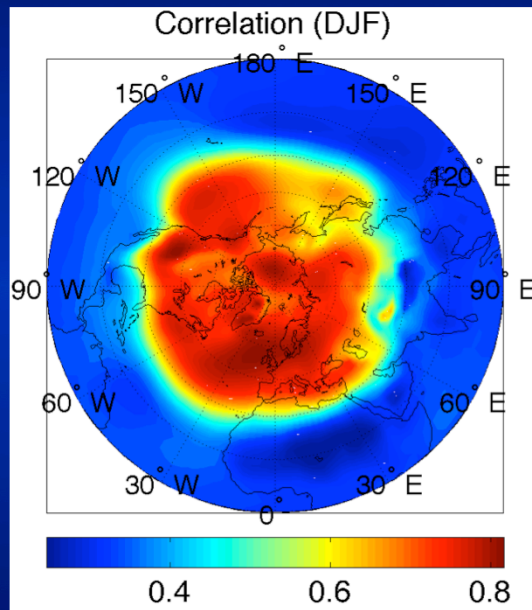
Example of a synoptically reconstructed time series (DJF)



- Correlations of about 0.7–0.8
- Similar LFV in actual and reconstructed series
- Similar results for other seasons (not shown)

In this slide we see a segment of the full vs. reconstructed SLP time series at an arbitrarily chosen mid-latitude location, with the time series of the full SLP in blue, and the synoptically reconstructed SLP in red. The reconstructed field exhibits high correlations of about 0.7–0.8 with the full-field time series and has a realistic magnitude. Quantitatively, it accounts for about 50% of the total SLP variance, but it also captures a larger fraction (of >80%) of the total variance for the low-pass filtered SLP field (not shown). This means that the synoptic reconstruction in fact captures most of the LFV present in the full SLP field!

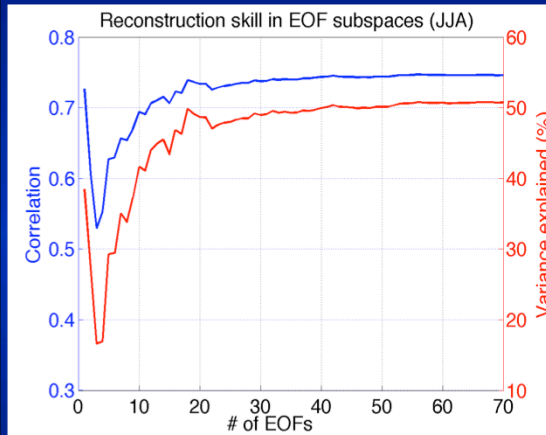
Synoptic reconstruction skill (DJF)



- High correlations of >0.7 north of 30°N
- Even higher correlations for low-pass filtered data (not shown)
- Same results for other seasons (not shown)

The results shown on the previous slide are valid basin-wide north of 30°N , where the correlations between the full and synoptically reconstructed SLP time series are generally higher than 0.7 and even higher for the low-pass filtered data, thereby indicating, once again, that our synoptic reconstruction captures well the LFV of the full SLP field.

Reconstruction skill in EOF subspaces



- Consider actual and reconstructed variability in the subspace of N leading EOFs of respective fields

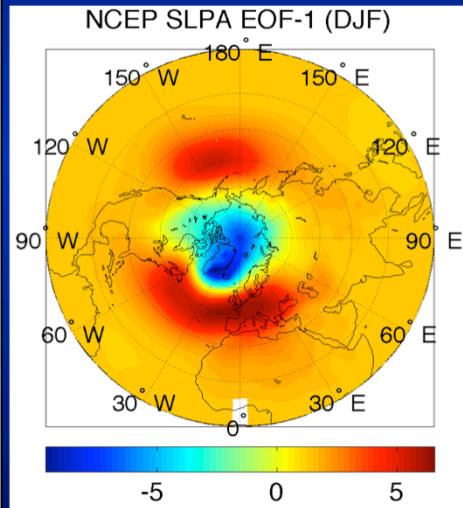
- Compute reconstruction skill (north of 30° N) for each N

- Result: skill saturates at $N \sim 30$ —

RECONSTRUCTION CAPTURES LFV ASSOCIATED WITH TELECONNECTIONS!

Another way of looking at the same result is to compare full and synoptically reconstructed SLP variability in the subspaces of leading N EOFs of the full and synoptically reconstructed fields, for different values of N . The procedure goes as follows. First, we compute the SVD decomposition of both actual and reconstructed fields, then truncate it to N leading modes and re-compute these truncated SLP fields in the physical space. Then we compute the correlations between time series of actual and reconstructed fields at each point in space, and find the average correlation north of 30° N. It turns out that the reconstruction skill saturates at ~ 0.7 for $N \sim 20-30$. This means that variability contained in the subspace of higher-order EOFs, beyond $N=30$, essentially adds nothing to the reconstruction skill. In other words, all of the useful skill is contained in the subspace associated with the leading 20–30 EOFs of the actual and reconstructed fields. Since this subspace contains, among other things, what's known as various teleconnection patterns, we arrive at the result that synoptic reconstruction captures the full-field low-frequency variability associated with teleconnections!

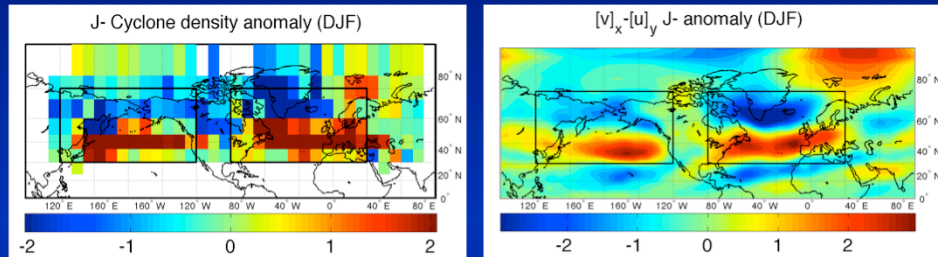
Leading EOF (AO) is well correlated with zonal-mean zonal wind $\langle[u]\rangle$ variability. **Next:**



- Use $\langle[u]\rangle$ leading PC as a zonal-jet proxy
- Compute composites of eddies over high-index (J+) and low-index (J-) zonal-jet states
- Compute cross-spectra of eddies and zonal jet

The leading teleconnection pattern is associated with the mode of variability known as Arctic Oscillation, or the Northern Annual Mode (NAM). It is also well correlated with the zonal-index variability in the Northern Hemisphere, computed as the leading principal component of the zonally and vertically averaged zonal wind. Next we will try to isolate changes in the characteristics of individual eddy lifecycles during various phases of the zonal-index variability and comment on causality in the zonal-jet/synoptic eddies symbiotic system.

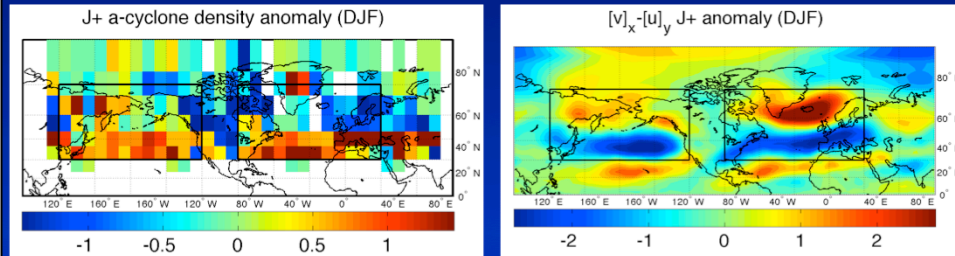
Composites of cyclone density and relative vorticity in low-index state



- Shown are anomalies with respect to climatology (DJF)
- **Positive** spatial correlation (~ 0.7) btw vorticity and **cyclone** density anomalies

The quantity that exhibits most dramatic changes in the course of the zonal-index variability is the spatial density of the cyclones and anticyclones (the quantity essentially related to an average number of cyclone or anticyclone tracks passing through a given region). Shown in the left panel is the cyclone density composite anomaly in the low-index zonal-jet state, with respect to climatology. The graph in the right panel is for the composite anomaly of the vertically averaged relative vorticity in the low-index jet state. The two fields are well correlated (spatial correlation of ~ 0.7), which shows that the regions of positive relative vorticity anomaly are also the regions with more cyclones than in the climatological state and vice versa (the regions of negative relative anomaly are also the regions with fewer cyclone tracks than in the climatological state).

Anticyclone density and relative vorticity anomalies in high-index state

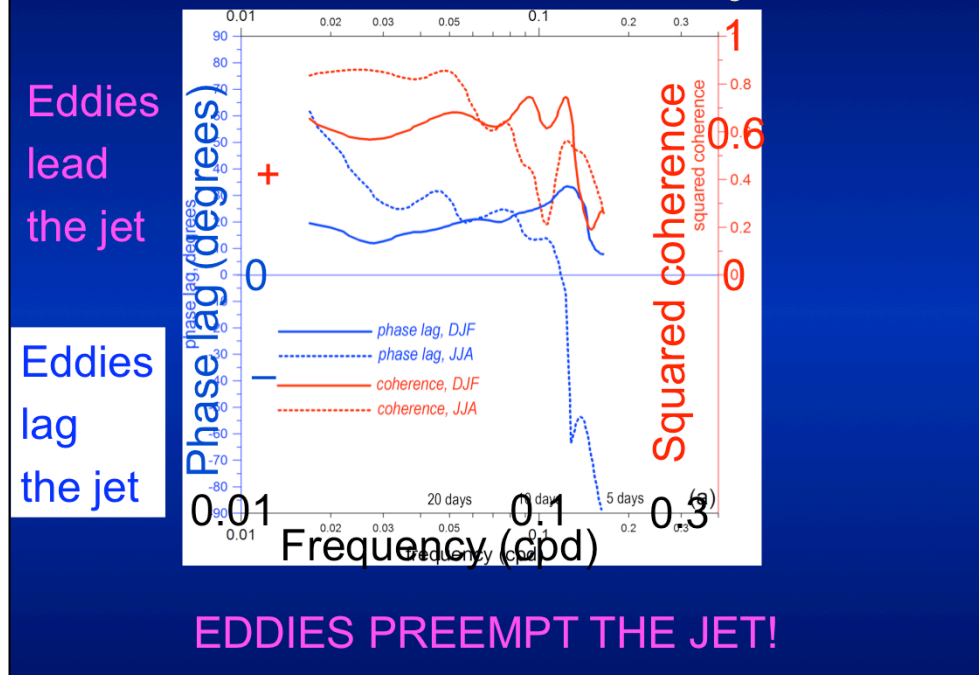


- Negative spatial correlation (~ -0.6) btw vorticity and anticyclone density anomalies

ARE VORTICITY ANOMALIES IN JET-SHIFTED STATES DUE TO THE FACT THAT CYCLONE / A-CYCLONE NUMBERS CHANGE OR VICE VERSA?

An analogous association applies to anticyclone tracks too. Here we show the anticyclone density and relative vorticity composite anomalies in the high-index jet state, which exhibit a negative spatial correlation. In both cases of cyclones and anticyclones, we thus see the association, at very low frequencies, between the number of cyclone (positive vorticity anomaly feature) and anticyclone (negative vorticity anomaly feature) tracks in a given region and this region's relative vorticity anomaly. In particular, a positive vorticity anomaly in the region is associated with more cyclones and fewer anticyclones straddling this region and vice versa. The central question then becomes the one of causality: Are the larger-scale relative vorticity anomalies due to changes in the number of regional cyclone/anticyclone tracks or, conversely, are the cyclone/anticyclone regional density anomalies the result of a large-scale preconditioning associated with an inherently large-scale low-frequency variability?

Storm-track latitude and jet shifts



To address this question, we created a proxy time series of the storm-track variability based on the output of the tracking procedure. We saw previously, in the composite anomalies of cyclone/anticyclone densities, that the leading pattern of variability for cyclone and anticyclone tracks connected to the jet shifts is also largely zonally symmetric and is characterized by the meridional displacement of eddy activity. An average latitude of cyclones and anticyclones is thus a reasonable proxy for this behavior. We created the time series of this quantity, for cyclones and anticyclones separately, and performed a cross-spectrum analysis of the cyclone or anticyclone latitude time series and the zonal-index time series. The results of this analysis (see the slide) indicate that eddies tend to lead the jet throughout the entire spectral range and throughout the year, perhaps with the exception of high-frequency anomalies in summer.

This is a bit surprising and is in contradiction with the results of analogous reconstruction in a baroclinic channel QG model, where eddies lead the jet variability at high frequencies, but also *lag* the jet variability at low frequencies. We are still contemplating about what the observational results really mean and why they are different from QG predictions, but the current conclusion is that the jet-index variability is synonymous with the storm-track variability and merely represents the ultra-low-frequency

Summary

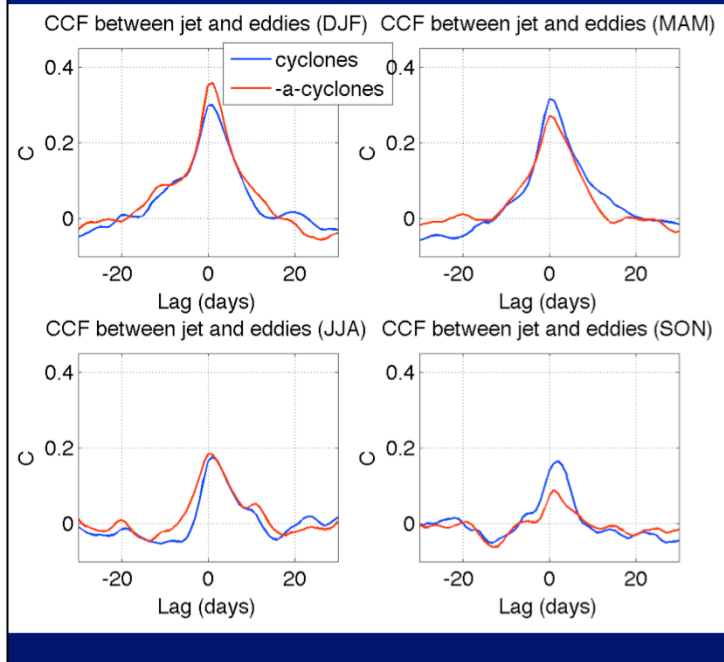
- **Synoptically reconstructed fields** were obtained by approximating local SLP minima and maxima, for each NCEP snapshot, with **round Gaussian “cyclones” and “anticyclones”**
- The synoptic field so reconstructed reproduces **~50% of total variability, including LFV of teleconnection patterns**. The remaining 50% are thus due to mesoscale features associated with axial asymmetries of cyclones and anticyclones
- **Cyclone / anticyclone spatial density anomalies preempt the vorticity** anomalies associated with zonal-index variability, **at all frequencies!**

In summary, we've developed a scheme for isolating the synoptic component of sea-level pressure field using the output of the cyclone/ anticyclone tracking procedure and reconstructing this synoptic field for each time by superimposing Gaussian patches of low- and high-pressure anomalies associated with each cyclone and anticyclone. The main advantages of this scheme over a traditional high-pass time filtering are that it keeps immediate connection with the features directly observed in the snapshots of SLP fields and avoids aliasing inherent in the time-filtering schemes due to the absence of the clear time scale separation between synoptic eddies and low-frequency flow. The synoptic reconstruction accounts for a surprisingly large fraction of the total SLP variability, and, even more surprisingly, best captures the low-frequency variability associated with teleconnection patterns. Finally, the cross-spectral analysis of the zonal-index and eddy-latitude time series indicates that the synoptic eddies lead the jet at all frequencies, which seems to suggest that the zonal-index variability is but a random ultra-low-frequency redistributions of the cyclone and anticyclone trajectories. This result still needs fleshing out, especially due to apparent mismatch with QG-model predictions.

Select references

- Barnes, E. A., and D. L. Hartmann, 2010: Dynamical feedbacks and persistence of the NAO. *J. Atmos. Sci.*, **67**, 851–865.
- Kravtsov, S., and S. Gulev, 2013: Kinematics of Eddy–Mean Flow Interaction in an Idealized Atmospheric Model. *J. Atmos. Sci.*, **70**, 2574–2595.
- Löptien, U., and E. Ruprecht, 2005: Effect of synoptic systems on the variability of the North Atlantic Oscillation. *Mon. Wea. Rev.*, **133**, 2894–2904.
- Rudeva, I., and S. K. Gulev, 2011: Composite Analysis of North Atlantic Extratropical Cyclones in NCEP–NCAR Reanalysis Data. *Mon. Wea. Rev.*, **139**, 1419–1446.
- Vallis, G. K., and E. P. Gerber, 2008: Local and hemispheric dynamics of the North Atlantic oscillation, annular patterns and the zonal index. *Dyn. Atmos. Oceans*, **44**, 184–212.

Storm-track latitude and jet shifts-1



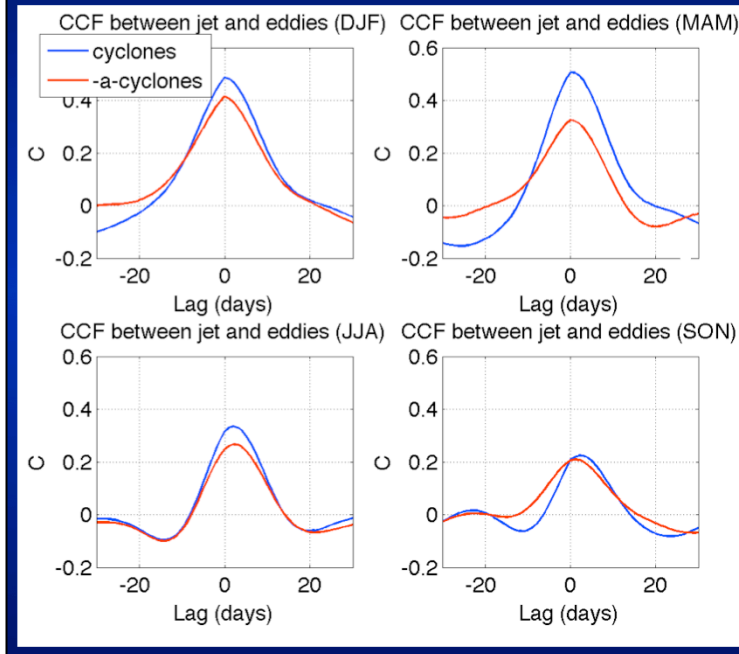
Positive lags:
Eddies lead
the jet

It appears
that cyclone/
anticyclone
anomalies
preempt jet
shifts!

The next three slides (including this one) are add-on slides.

This slide summarizes the results of the cross-correlation analysis between the time series of the cyclone or anticyclone latitude and the zonal-index time series at various lags. These correlations are shown here, for all seasons, with blue lines representing the correlations between the cyclone-latitude time series and zonal index, and red lines — the correlations between the anticyclone latitude time series multiplied by minus 1 and zonal index. The positive lags correspond to the eddy time series leading the jet. The main result of this exercise is most clearly obvious for the summer season, but in fact applies to all seasons too: the cross-correlation function is asymmetric and has a slower decay at positive lags, thus indicating that the cyclone/anticyclone latitude time series is leading the zonal-index time series. This behavior may be expected at the high-frequency end of the spectrum, where the redistribution of the cyclone and anticyclone tracks leads to the the mid-latitude jet displacements. However (next slide), we find the same lead-lag relationship between the jet and eddies at low frequencies too. See also the cross-spectrum analysis slide of the main part of the presentation.

Storm-track latitude and jet shifts-2

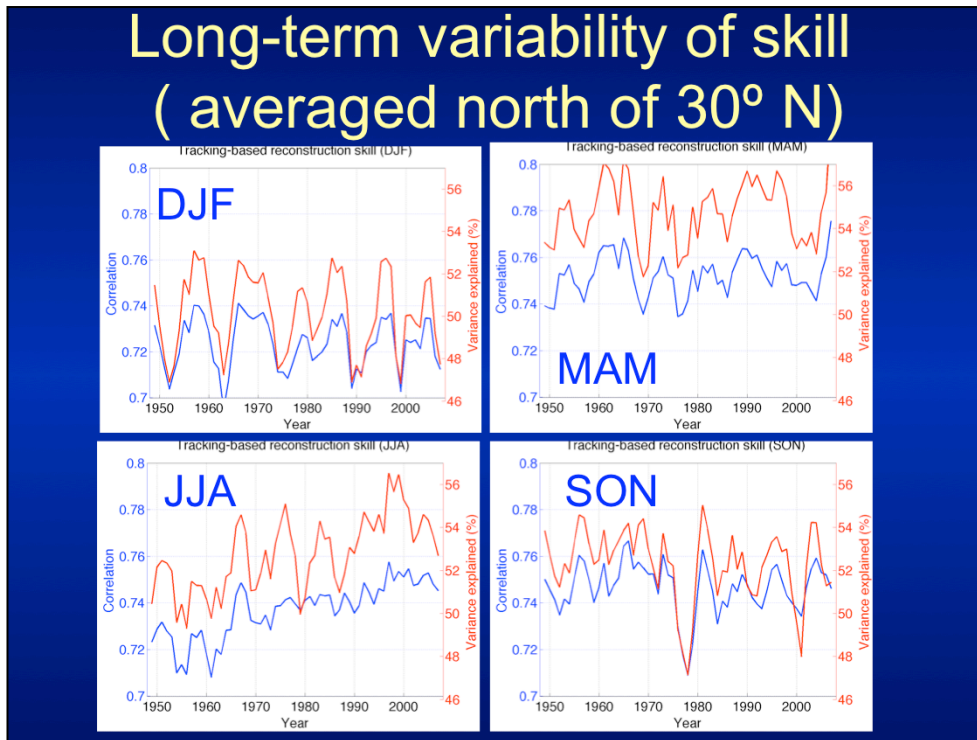


It appears that cyclone/anticyclone anomalies preempt jet shifts...

... for low-pass filtered data too!

This slide is analogous to the previous one, but shows the cross-correlations between low-pass filtered versions of the eddy-latitude and zonal-index time series. Once again, we see higher correlations at positive lags corresponding to the eddies leading the mid-latitude jet displacements. This is also explicitly confirmed by the cross-spectrum analysis of the eddy-latitude and zonal-index time series (not shown), which reveals that the eddy time series leads the jet time series at all frequencies, while the squared coherence remains small for high frequencies and increases to a value of about 0.2–0.3 for lower frequencies (corresponding to the maximum cross-correlations of 0.4–0.5 consistent with the values in this slide).

Long-term variability of skill (averaged north of 30° N)



This is an aside slide, which shows interesting decadal variability of the synoptic-reconstruction skill, with pronounced quasi-periodic decadal signal in winter, pronounced trend in summer, as well as drop of skill in fall 1978, at the time known as the “climate shift of the 70s,” and secondary drop in 2001, also a time of a climate regime change according to some authors.